Figure S1

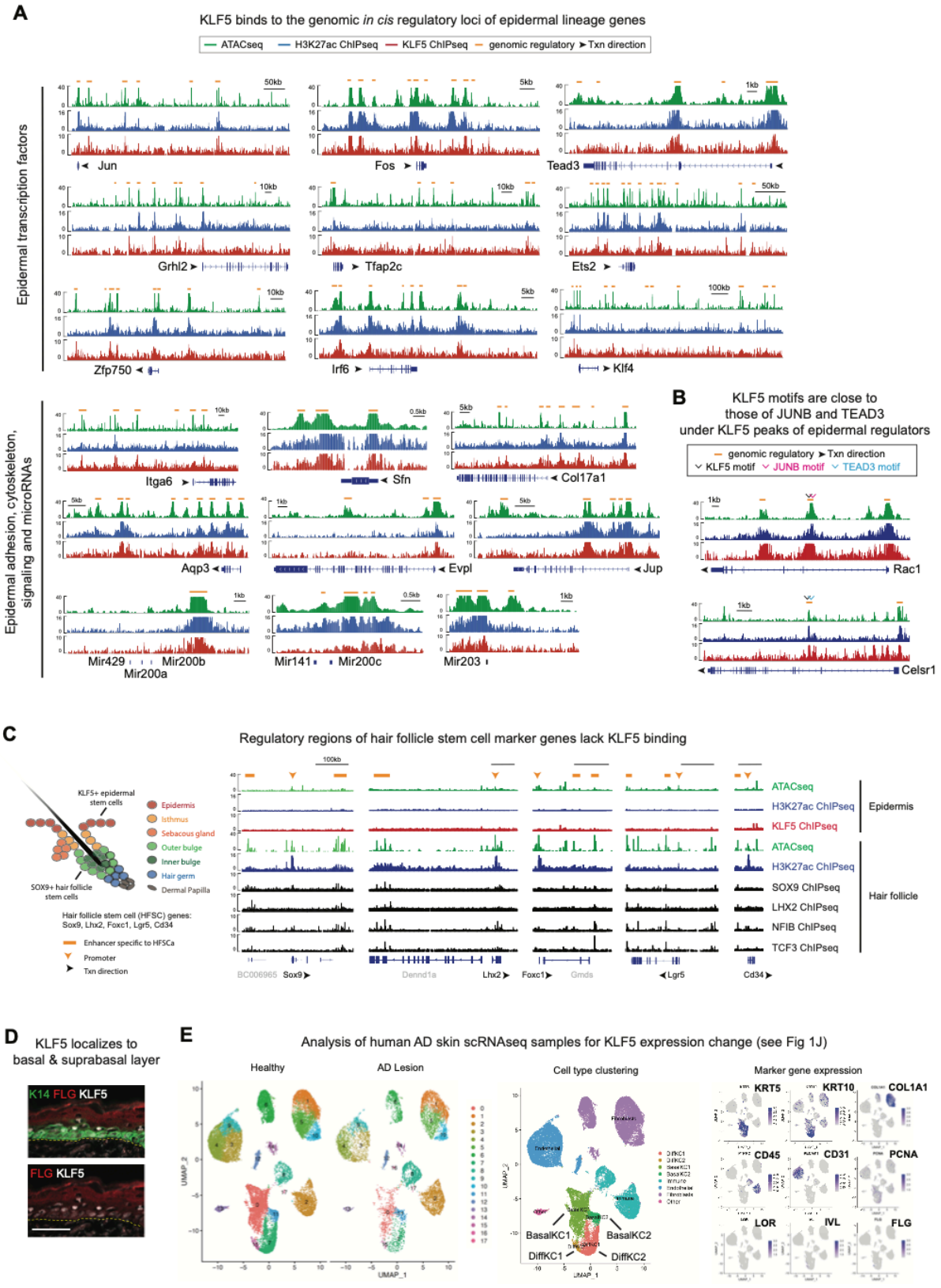

Figure S1. KLF5 is a master epidermal lineage regulator

(A-B) ATACseq (green), H3K27ac ChIPseq (blue), and KLF5 ChIPseq (red) tracks showing KLF5-associated putative regulatory elements (denoted as orange lines on top of the tracks) of selected epidermal TFs (Jun, Fos, Tead3, Grhl2, Tfap2a (encoding AP2g), Ets2, Zfp750 (encoding ZNF750), Irf6, Klf4), epidermal adhesion and signaling (Itga6, Sfn, Col17a1, Egfr), stratification and cornified envelope (Aqp3, Evpl, Jup), and epithelial

microRNAs (miR-429-200a/b, miR-141-200c, miR-203). Gene annotation tracks (major isoform represented) are shown underneath, with taller boxes indicating coding sequence exons, shorter boxes indicating untranslated region exons, and lines indicating introns. Arrows next to gene names indicate direction of transcription (txn), shown for individual gene tracks. In (B), color-coded open arrow heads denote JUNB and TEAD3 motifs adjacent to KLF5 motifs under KLF5 peaks associated with Rac1 and Celsr1 genes.

(**C**) ATACseq (green), H3K27ac ChIPseq (blue) and KLF5 ChIPseq (red) profiled in epidermal stem cells in comparison to ATACseq (green), H3K27ac ChIPseq (blue), and SOX9/LHX2/NFIB/TCF3 (known hair follicle stem cell TFs) ChIPseq (black) profiled in hair follicle stem cells. Black lines on top of the tracks denote hair follicle stem cell specific enhancers regulating expression of known markers of hair follicle stem cells including *Sox9, Lhx2, Foxc1, Lgr5, Cd34*, all of which lack KLF5 binding in the epidermis.

(D) IF images show KLF5 is specifically expressed in the basal and suprabasal but not granular (non-overlap with FLAGGRIN, FLG) layers. Yellow dashed lines mark epidermal-dermal border. Bar, 50 μm. Images are representative and from at least 5 biologically independent replicates.

(E) scRNAseq for skin from atopic dermatitis (AD) patients and healthy donor, showing cell population assignments based on marker gene expression (related to Fig 1J).

Related to Figure 1.

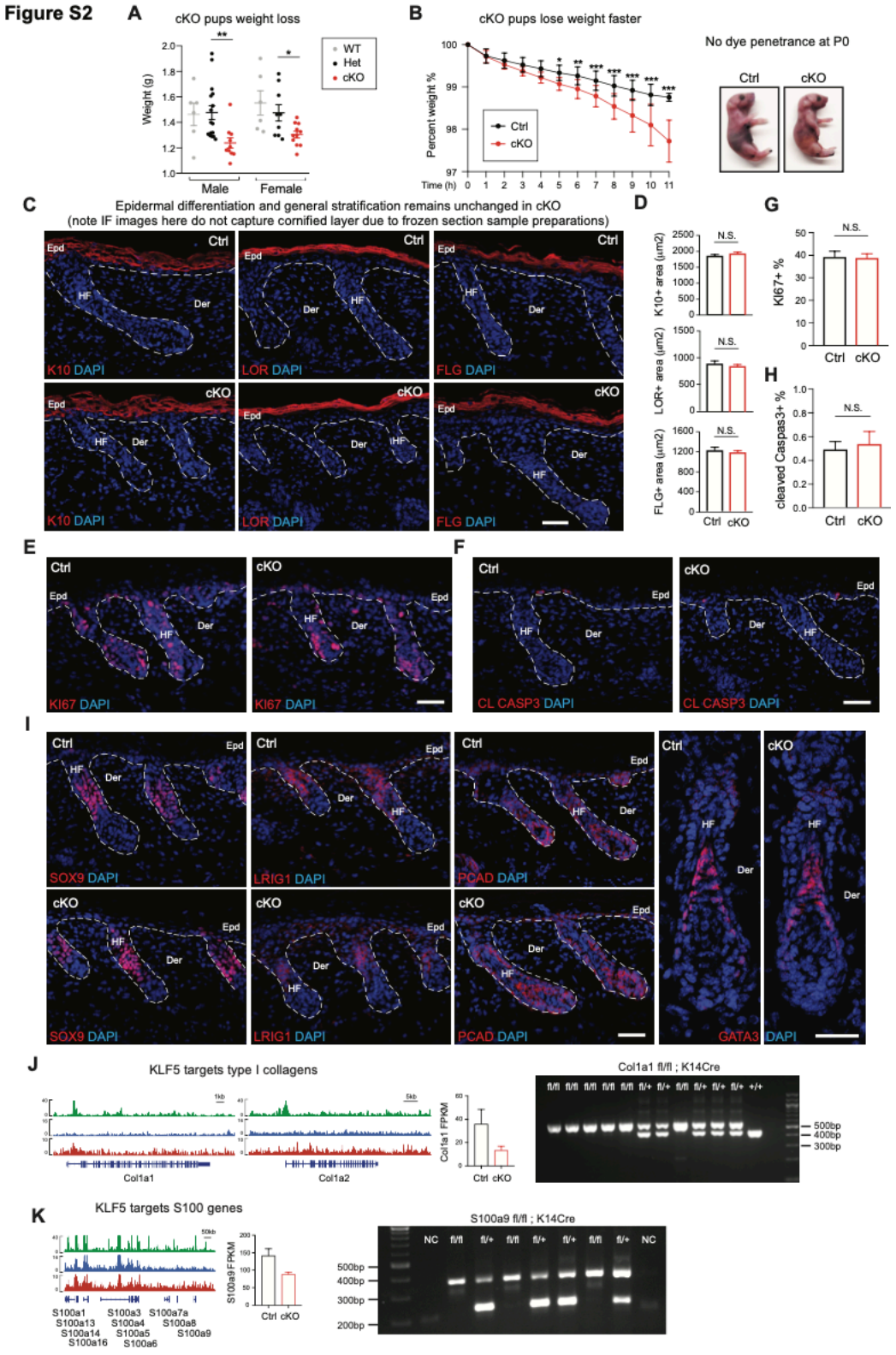

Figure S2. KLF5 ablation does not substantially affect epidermal differentiation, proliferation, apoptosis, or hair follicle morphogenesis

All images are representative and from at least 5 biologically independent replicates. White dashed lines on immunofluorescence (IF) images denote the epidermal-dermal border. Epd, epidermal. HF, hair follicle. Der, dermis. cKO, *Klf5*$^{fl/fl}$*; K14Cre*+ epidermal-specific knockout mice. Ctrl, *Klf5*$^{fl/+}$*; K14Cre*+ heterozygous control mice. Epd, epidermis. HF, hair follicle. Der, dermis.

(A) Weight measurements at postnatal day 0 (p0) demonstrate Klf5 conditional knockout (cKO) mice are significantly smaller compared to heterozygous (Het) and WT groups, true in both sexes.

(B) Hourly weight measurements at p0 reveal cKO lose weight more rapidly than Ctrl littermates (Ctrl n=13, cKO n=14). Toluidine Blue O dye exclusion assay shows at birth, both Ctrl and surviving cKO are able to exclude dye.
(C-D) Immunofluorescence staining and quantifications of epidermal differentiation markers keratin 10 (K10), loricrin (LOR) and filaggrin (FLG) in Ctrl and cKO at p0, with no significant changes (n=8 for K10 both groups; n=7 for LOR both groups; Ctrl n=6, cKO n=8 for FLG). Bar, 50 μm.
(E, G) IF staining and quantification of the proliferation marker Ki67 in Ctrl and cKO at p0 (n=6 for both groups), showing no significant changes. Bar, 50 μm.
(F, H) IF staining and quantification of the apoptosis marker cleaved caspase-3 in Ctrl and cKO at p0 (n=6 for both groups), showing no significant changes. Bar, 50 μm.
(I) IF staining of hair follicle morphogenesis markers SOX9, LRIG1, P-cadherin (PCAD) and GATA3 in Ctrl and cKO at p0, showing no significant changes. Bar, 50 μm for SOX9, LRIG1 and PCAD. Bar, 10 μm for GATA3.
(J) Left: ATACseq (green), H3K27ac ChIPseq (blue), and KLF5 ChIPseq (red) tracks showing KLF5 putative target *Col1a1* (and its partner Col1a2). *Col1a1* transcriptional level is reduced in *Klf5* cKO. Right: genotyping gels showing floxed alleles from *Col1a1$^{fl/fl}$; K14Cre+* animals.
(K) Left: ATACseq (green), H3K27ac ChIPseq (blue), and KLF5 ChIPseq (red) tracks showing KLF5 putative target *S100a9* (and its residing genomic locus encompassing the cluster of S100 genes). *S100a9* transcriptional level is reduced in *Klf5* cKO. Right: genotyping gels showing floxed alleles from *S100a9$^{fl/fl}$; K14Cre+* animals.
Unpaired t-tests were performed for (A), (D), (G), (H). Two-way analysis of variance (ANOVA) with repeated measurement was performed for (B). *$p<0.05$, **$p<0.01$, ***$p<0.001$. Data are mean ± SEM. N.S., not significant.
Related to Figure 2

Figure S3

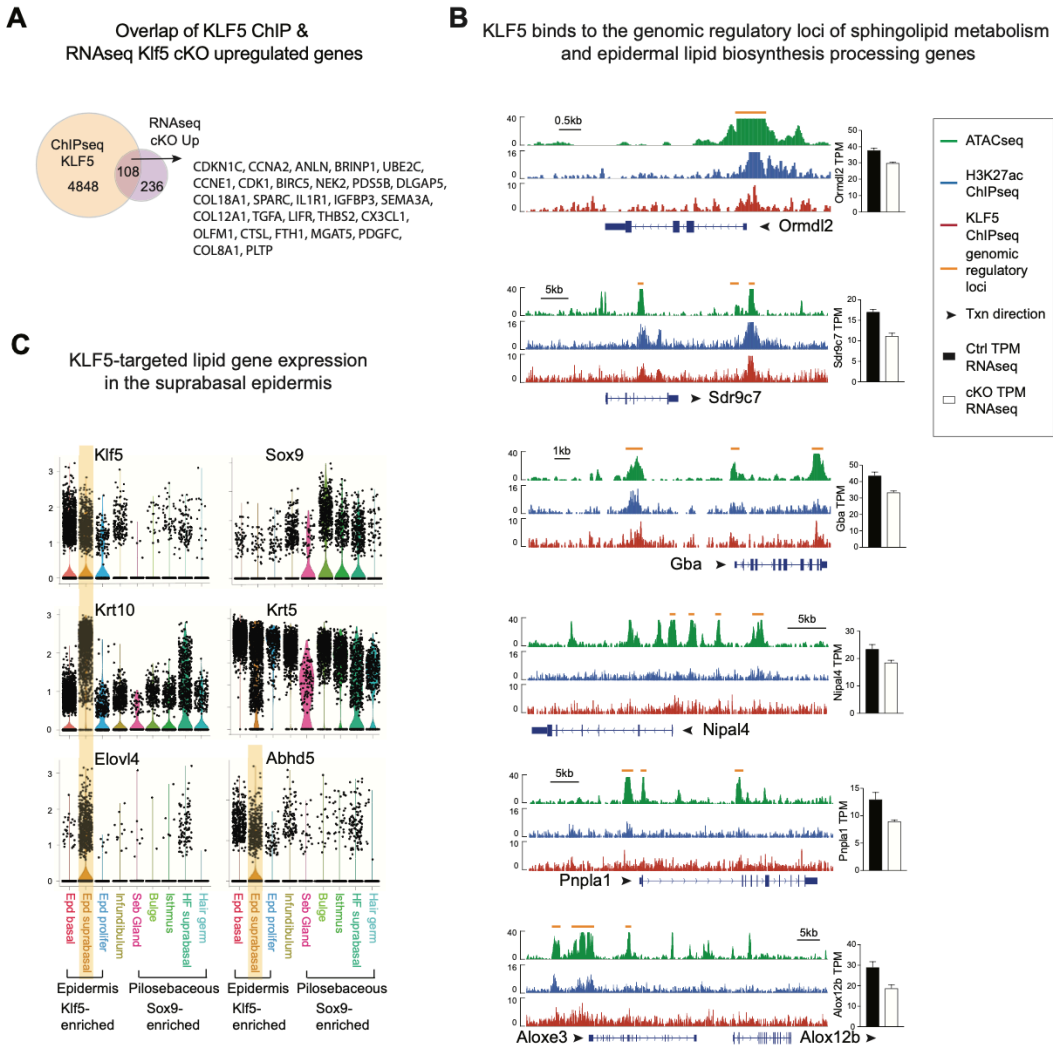

Figure S3. Lipid metabolism genes are differentially expressed in cKO verses Ctrl

(A) Venn diagram overlapping KLF5 ChIPseq peaks (KLF5 bound genes) with Klf5 cKO induced genes. A list of cell adhesion and signaling genes within the overlap are shown.

(B) ATACseq (green), H3K27ac ChIPseq (blue), and KLF5 ChIPseq (red) tracks showing KLF5 putative targets in sphingolipid metabolism pathway. Gene annotation tracks (major isoform represented) are shown underneath, with taller boxes indicating coding sequence exons, shorter boxes indicating untranslated region exons, and lines indicating introns. Arrows next to gene names indicate direction of transcription (txn), shown for individual gene tracks.

(C) Violin plots of scRNAseq data showing transcriptional levels of Klf5 (epidermis), Sox9 (pilosebaceous unit including sebaceous gland and hair follicle), Krt10 (highest in suprabasal epidermis), Krt5 (basal layer of the skin epithelia), along with Klf5 targets Elovl4 and Abhd5 (both enriched in suprabasal epidermis).

Related to Figure 3

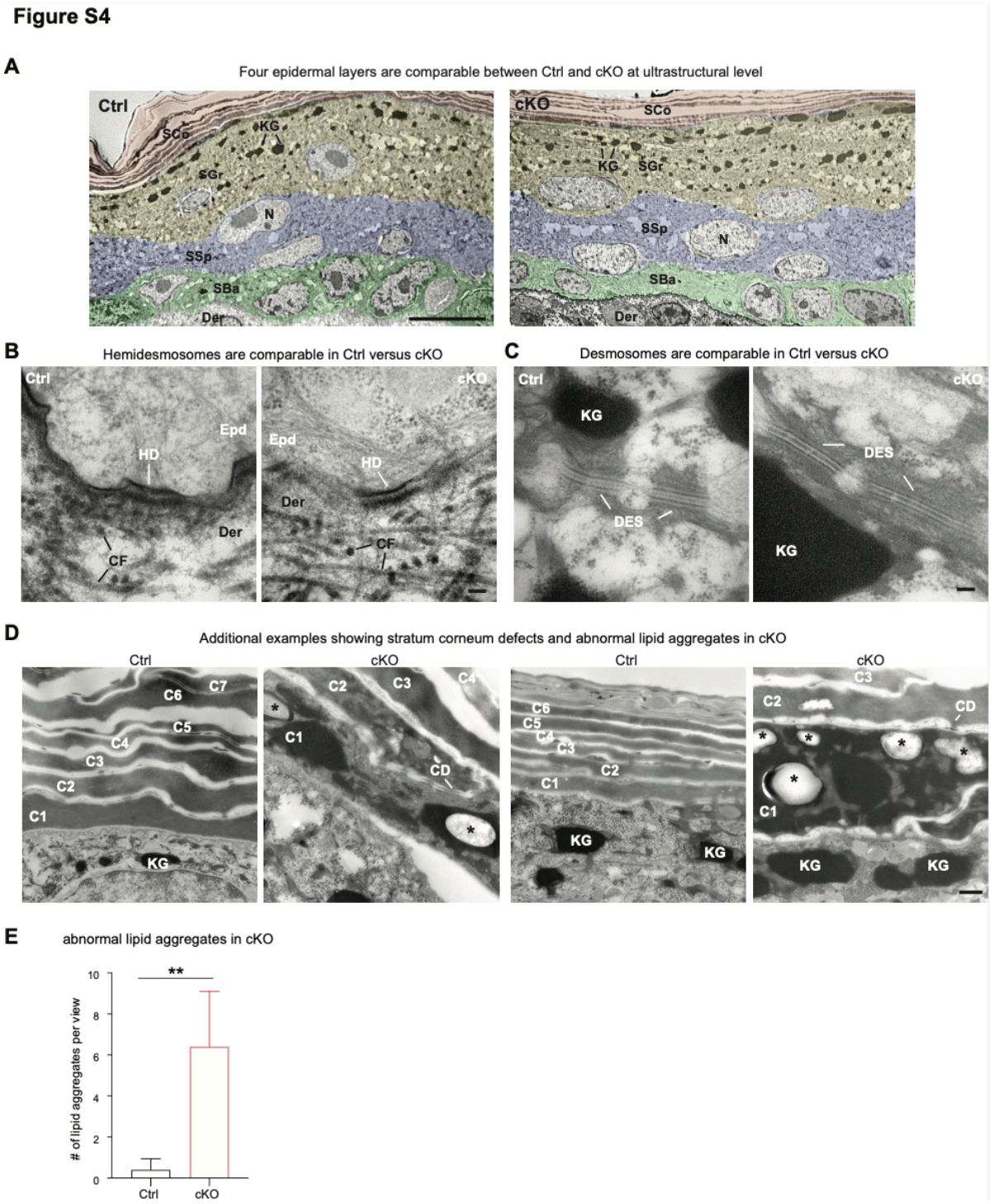

Figure S4. KLF5 ablation does not affect epidermal junctions but leads to accumulated of lipid aggregates and disrupted stratum corneum

(A) Transmission electron microscopy (TEM) at 2000× magnification provides an overview of the four epidermal layers of stratum basale (SBa), stratum spinosum (SSp), stratum granulosum (SGr) and stratum corneum (SCo), which appear similar between Ctrl and cKO mice. N, nucleus. Der, dermis. KG, keratohyalin granules. Bar, 10 μm.

(B) Transmission electron microscopy (TEM) at 100,000× magnification shows well-organized hemidesmosomes (HD) connecting basement membrane and basal epidermal stem cells in both Ctrl and cKO samples. Epd,

epidermis. Der, dermis. CF, collagen fibers at both cross-orientation and longitudinal orientation. KG, keratohyalin granules. Bar, 100 nm.
(C) TEM at 100,000× magnification shows well-organized desmosomes (DES) connecting 2 adjacent epidermal cells of the granular layer in both Ctrl and KO samples. KG, keratohyalin granules. Bar, 100 nm.
(D) TEM at 25,000× magnification shows a range of phenotypic severities of cKO epidermis including disorganized cornified envelope and appearance of lipid clusters. Asterisks (*) denote abnormal lipid aggregates found in the cKO stratum corneum, reminiscent of case reports from skin congenital disorder patients with barrier defects. CD, corneodesmosome. C1 denotes the first layer of cornified envelope in both Ctrl and cKO. KG, keratohyalin granules. Bar, 500 nm.
(E) Quantification of abnormal lipid aggregates in Ctrl and cKO epidermis. n=6 for Ctrl and cKO **$p<0.01$, Data are mean ± SEM.
Related to Figure 4

Figure S5

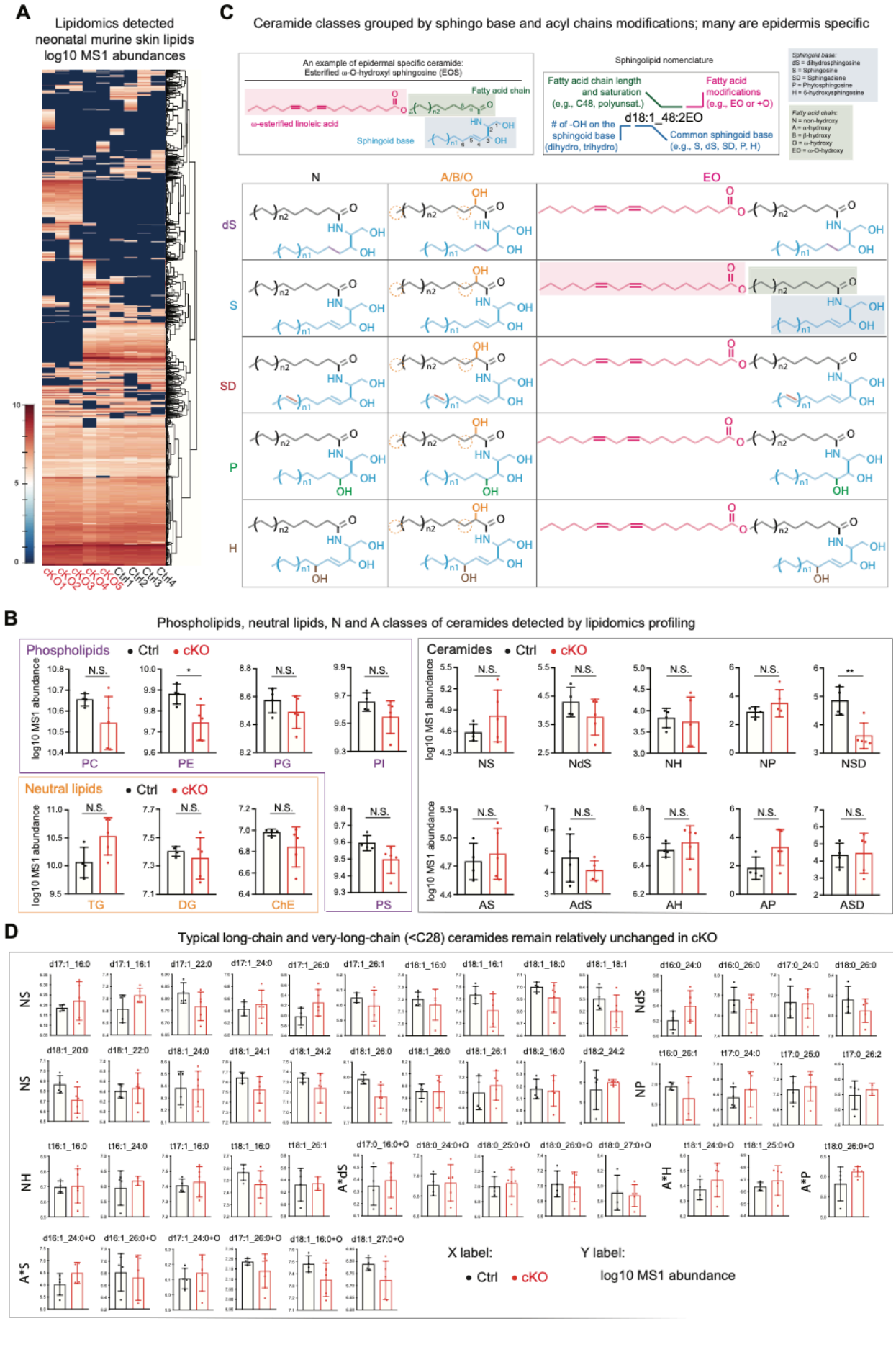
A
Lipidomics detected neonatal murine skin lipids log10 MS1 abundances
cKO1
cKO2
cKO3
cKO4
cKO5
Ctrl1
Ctrl2
Ctrl3
Ctrl4
C
Ceramide classes grouped by sphingo base and acyl chains modifications; many are epidermis specific
An example of epidermal specific ceramide: Esterified ω-O-hydroxyl sphingosine (EOS)
Fatty acid chain
ω-esterified linoleic acid
Sphingoid base
Sphingolipid nomenclature
Fatty acid chain length and saturation (e.g., C48, polyunsat.)
Fatty acid modifications (e.g., EO or +O)
d18:1_48:2EO
of -OH on the sphingoid base (dihydro, trihydro)
Common sphingoid base (e.g., S, dS, SD, P, H)
Sphingoid base:
dS = dihydrosphingosine
S = Sphingosine
SD = Sphingadiene
P = Phytosphingosine
H = 6-hydroxysphingosine
Fatty acid chain:
N = non-hydroxy
A = α-hydroxy
B = β-hydroxy
O = ω-hydroxy
EO = ω-O-hydroxy
N
A/B/O
EO
dS
S
SD
P
H
B
Phospholipids and neutral lipids, N and A classes of ceramides detected by lipidomics profiling
Phospholipids
Ctrl
cKO
log10 MS1 abundance
N.S.
PC
PE
PG
PI
Neutral lipids
TG
DG
ChE
PS
Ceramides
NS
NdS
NH
NP
NSD
AS
AdS
AH
AP
ASD
D
Typical long-chain and very-long-chain (<C28) ceramides remain relatively unchanged in cKO
NS
NdS
NP
NH
A*dS
A*H
A*P
A*S
X label:
Ctrl
cKO
Y label:
log10 MS1 abundance

Figure S5. Lipidomics profiling detected > 2200 lipid species in the neonatal murine skin

(A) Lipidomics profiling was performed on skin samples of p0 heterozygous controls (Ctrl, black, n=4) or Klf5 conditional knockout mice (cKO, red, n=5). Unsupervised clustering showing log10-transformed mass spectrometry (MS1) abundance of 2265 detected lipid species (detected at least in 1 sample).

(B) Lipid class-level analysis comparing Ctrl and cKO. Log10-transformed mass spectrometry (MS1) abundance of detected lipid species is plotted on the y-axis. The phospholipids phosphatidylcholine (PC), phosphatidylglycerol (PG), phosphatidylinositol (PI), phosphatidylserine (PS) was unchanged, and phosphatidylethanolamine (PE) was reduced. Neutral lipids including triglycerides (TG), diglycerides (DG), and cholesterol ester (ChE) remained unchanged. Among ceramides, non-hydroxy (N) and α-hydroxy (A) classes were unchanged as a group. Data are mean ± SD. *$p<0.05$, **$p<0.01$, N.S. not significant.

(C) Nomenclature and chemical structure of ceramide classes: An example of esterified ω-O-hydroxy sphingosine (EOS) is shown, a unique epidermal acylceramide with C18:2 linoleic acid esterified to the ω-O position of the acyl chain. Based on ceramide nomenclature, the beginning letter(s) denote the hydroxyl modification of fatty acid acyl chain (N, non-hydroxy; A, α-hydroxy; B, β-hydroxy; O, ω-hydroxy; EO, ω-O-hydroxy), and the ending letter(s) denote the sphingoid base (dS, dihydrosphingosine; S, sphingosine; P, phytosphingosine; H, 6-hydroxysphingosine; SD, sphingadiene). On the sphingoid base, carbon position #1/#3 and carbon position #2 are invariable with hydroxyl group and amide group, respectively. The carbon position #4-#6 determines the type of sphingoid base (S has double bond between C4 and C5, P has hydroxyl group at C4, H has hydroxyl group at carbon C6). n1 and n2 are determined based on the carbon numbers of the sphingoid base and acyl chain, respectively.

(D) Long-chain and very-long-chain (<C28) ceramides were unchanged between Ctrl and cKO. Data are mean ± SD. All comparisons shown were not significant based on unpaired t test. This result is consistent with our lipid class level analysis showing that as a group, the ceramide class was moderately reduced in cKO. While the majority of ceramides remained relatively unaffected, a selective group of acylceramides (EO class) as well as ultra-long-chain ceramides were preferentially reduced in cKO as shown in main figure.

Related to Figure 5

Figure S6

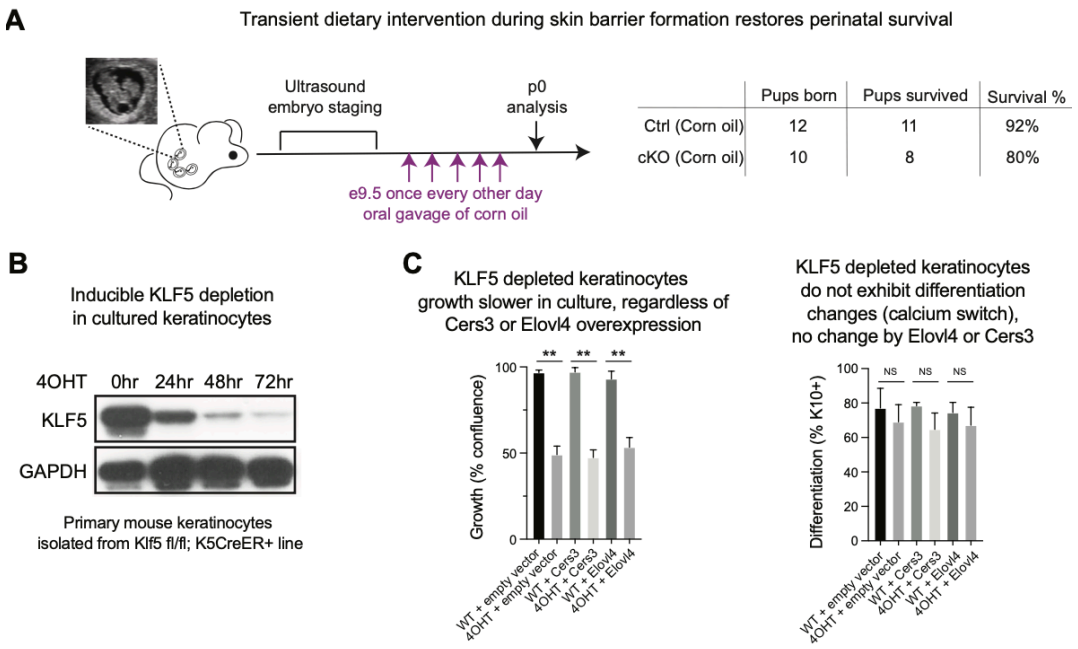

Figure S6. Dietary supplement of corn oil enriched with linoleic acid via oral gavage restored cKO survival
(A) Left: schematics showing transient dietary intervention regimen. Pregnant dam was subjected to embryonic staging via ultrasound every two to three days once bred starts, and until e9.5 was identified, upon which point the female was administrated with corn oil one-time via oral gavage. 10 days later, pups were born, and survival was recorded. Right: one litter was collected, and all pups survived regardless of Ctrl or cKO.
(B) Primary keratinocyte culture derived from Klf5 fl/fl; K5CreER (icKO) or Klf5 fl/+; K5CreER (Ctrl) skin epidermis. 5uM 4OHT was added to the culture media to induce KLF5 depletion and cell lysates were subjected to KLF5 and GAPDH WB.
(C) Elovl4 and Cers3 were cloned into lentiviral expression vector and expressed in icKO or Ctrl primary keratinocytes. Growth (% of confluence after two days of seeding in 25uM Calcium keratinocyte culture media and differentiation (% of K10+ cells two days after switching to 1.5mM calcium keratinocyte culture media) were analyzed. N = 3. Paired t test was performed. *$p<0.05$. NS = not significant.
Related to Figure 6

Figure S7

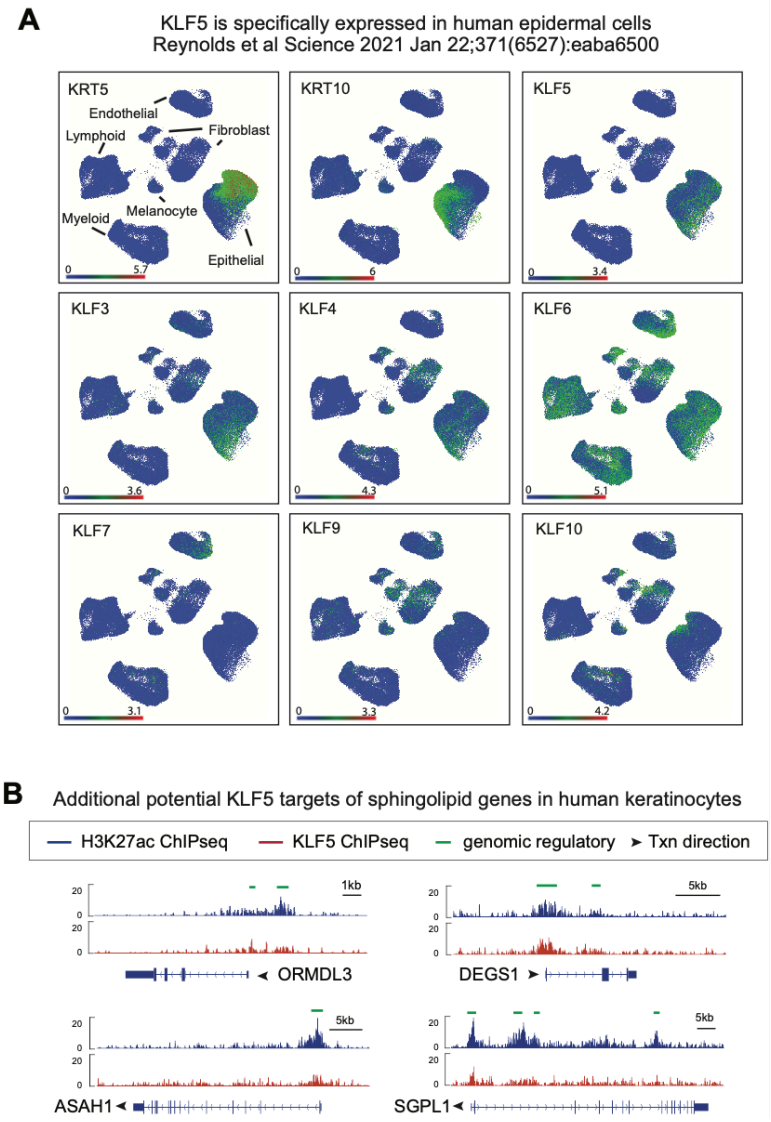

Figure S7. KLF5 function is conserved in human skin

(A) Publicly available healthy human skin scRNAseq data plotted using UMAP (Uniform Manifold Approximation and Projection) depicting the specific expression of KLF5 in KRT5+ or KRT10+ epidermal cells. In contrast, other KLF family members exhibit expressions in other cell types.

(B) H3K27ac ChIPseq (blue) and KLF5 ChIPseq (red) tracks showing KLF5-associated putative regulatory elements (denoted as green lines on top of the tracks) of selected sphingolipid metabolism genes in cultured human keratinocytes.

Related to Figure 7